



UvA-DARE (Digital Academic Repository)

Magnetic phases of two-component ultracold bosons in an optical lattice

Hubener, A.; Snoek, M.; Hofstetter, W.

Published in:
Physical Review B

DOI:
[10.1103/PhysRevB.80.245109](https://doi.org/10.1103/PhysRevB.80.245109)

[Link to publication](#)

Citation for published version (APA):

Hubener, A., Snoek, M., & Hofstetter, W. (2009). Magnetic phases of two-component ultracold bosons in an optical lattice. *Physical Review B*, 80(24), 245109. DOI: 10.1103/PhysRevB.80.245109

General rights

It is not permitted to download or to forward/distribute the text or part of it without the consent of the author(s) and/or copyright holder(s), other than for strictly personal, individual use, unless the work is under an open content license (like Creative Commons).

Disclaimer/Complaints regulations

If you believe that digital publication of certain material infringes any of your rights or (privacy) interests, please let the Library know, stating your reasons. In case of a legitimate complaint, the Library will make the material inaccessible and/or remove it from the website. Please Ask the Library: <http://uba.uva.nl/en/contact>, or a letter to: Library of the University of Amsterdam, Secretariat, Singel 425, 1012 WP Amsterdam, The Netherlands. You will be contacted as soon as possible.

Magnetic phases of two-component ultracold bosons in an optical lattice

A. Hubener,¹ M. Snoek,^{1,2} and W. Hofstetter¹¹*Institut für Theoretische Physik, Johann Wolfgang Goethe-Universität, 60438 Frankfurt am Main, Germany*²*Institute for Theoretical Physics, Valckenierstraat 65, 1018 XE Amsterdam, The Netherlands*

(Received 14 February 2009; revised manuscript received 22 October 2009; published 11 December 2009)

We investigate spin-order of ultracold bosons in an optical lattice by means of dynamical mean-field theory. A rich phase diagram with anisotropic magnetic order is found, both for the ground state and at finite temperatures. Within the Mott insulator, a ferromagnetic to antiferromagnetic transition can be tuned using a spin-dependent optical lattice. In addition we find a supersolid phase, in which superfluidity coexists with antiferromagnetic spin order. We present detailed phase diagrams at finite temperature for the experimentally realized heteronuclear ⁸⁷Rb-⁴¹K mixture in a three-dimensional optical lattice.

DOI: [10.1103/PhysRevB.80.245109](https://doi.org/10.1103/PhysRevB.80.245109)

PACS number(s): 67.85.Hj, 67.60.Bc, 67.85.Fg

I. INTRODUCTION

Ultracold atoms in optical lattices give access to studies of quantum magnetism with unprecedented control and precision. Whereas efficient cooling of fermionic atoms in optical lattices remains an experimental challenge, mixtures of bosonic atoms can more easily be cooled to the relevant temperature scales, thus realizing the Bose-Hubbard model^{1,2} with multiple species. Indeed, recent experiments have already succeeded in loading a heteronuclear mixture into an optical lattice.³ The interaction between the two species has been addressed by means of a Feshbach resonance,⁴ which offers a direct way of mapping out the phase diagram as a function of the interspecies interaction strength. Moreover, superexchange processes have been directly observed in a mixture of two-component bosons.⁵

Whereas the phase diagram of spinless bosons is qualitatively well captured by Gutzwiller mean-field theory,⁶ for a multispecies system dynamical correlations are important, because they give rise to spin order. Previous theoretical studies have either discussed the weak tunneling limit^{7,8} or performed expansions around mean-field⁹ or the strong-coupling limit.^{10,11} Numerical nonperturbative methods are available in one spatial dimension,^{12,13} and quantum Monte Carlo simulations were very recently performed for two spatial dimensions.¹⁴ In this article we focus on the generic three-dimensional situation where dynamical mean-field theory (DMFT) has been established¹⁵ as a highly reliable, nonperturbative approach to strongly correlated fermionic quantum systems. Here we apply the bosonic version of DMFT (BDMFT), as recently introduced by Byczuk and Vollhardt.¹⁶ BDMFT treats condensed and normal bosons on equal footing. It is nonperturbative and hence can be applied within the full range from small to large couplings. The control parameter is the lattice coordination number z , i.e., the theory becomes exact in infinite dimensions. We present the BDMFT equations as a controlled $1/z$ expansion, up to sub-leading order. Our derivation is thus different from the original proposal,¹⁶ in which BMDFT is constructed as a well-defined theory in strictly infinite dimensions, which requires a different scaling of superfluid and normal parts of the action. In contrast, our derivation is based on a uniform scaling $\sim 1/z$ of the bosonic hopping amplitude. To leading order

this yields Gutzwiller mean-field theory,⁶ while from the sub-leading terms of order $O(1/z)$ we obtain the BDMFT equations. We thus regard BDMFT as an expansion in $1/z$ around Gutzwiller, which in our opinion is the most natural viewpoint.

In practice, BDMFT turns out to be an efficient and fast scheme, which allows to map out phase diagrams with high resolution. Moreover, it not only allows for nonperturbative calculation of local observables, but also the spectral function, relevant for RF spectroscopy, is directly accessible.

While in Ref. 16 calculations were only performed for a simplified lattice model with partially immobile bosons, here we apply bosonic DMFT to the full two-component Bose-Hubbard model in finite spatial dimensions. Besides the superfluid, we identify XY -ferromagnetic and Z -antiferromagnetic phases, in which translational symmetry is spontaneously broken and anisotropic magnetic order arises. Moreover, we find a supersolid phase where superfluidity coexists with antiferromagnetic spin order. We investigate the stability of these phases against thermal fluctuations, paying special attention to the experimentally relevant case of a heteronuclear ⁸⁷Rb-⁴¹K mixture in a three-dimensional optical lattice.³

II. METHOD

We first describe how BDMFT can be implemented for the Bose-Hubbard Hamiltonian. In particular we identify an Anderson Hamiltonian that reproduces the local effective action and allows us to solve the BDMFT self-consistency problem.

The starting point for our investigation is the multispecies single-band Hubbard model within tight-binding approximation

$$\hat{H} = - \sum_{\langle ij \rangle, \nu} (t_{\nu} \hat{b}_{i\nu}^{\dagger} \hat{b}_{j\nu} + \text{H.c.}) + \frac{1}{2} \sum_{i, \mu, \nu} U_{\nu\mu} \hat{n}_{i\nu} (\hat{n}_{i\mu} - \delta_{\nu\mu}), \quad (1)$$

which provides an accurate description of bosonic atoms in a sufficiently strong optical lattice. Here t_{ν} are (species-dependent) hopping amplitudes, $U_{\nu\mu}$ contains the inter- and intraspecies interactions and $\langle ij \rangle$ indicates a summation over nearest neighbor sites i and j . In the spirit of the cavity

derivation of the fermionic DMFT equations¹⁵ we consider a single lattice site (called the ‘‘impurity site’’) and formally integrate out all the other degrees of freedom. This defines the effective action of the impurity site as

$$Z_{\text{imp}} = \frac{Z}{Z^{(0)}} = \int \prod_{\nu} \mathcal{D}b_{0,\nu}^* \mathcal{D}b_{0,\nu} e^{-S_{\text{imp}}}, \quad (2)$$

where Z is the full partition function and $Z^{(0)}$ is the partition function of the cavity system without the impurity. For reasons of brevity we derive the effective impurity action and perform the numerical calculations in this article for the case of a Bethe lattice (Cayley tree), which in infinite dimensions ($z \rightarrow \infty$) has a semicircular density of states:¹⁵ $\rho_0(\epsilon) = \sqrt{4z^2 t^2 - \epsilon^2} / 2\pi z t^2$. The use of the semicircular DOS in our calculations has merely technical reasons because this choice simplifies the DMFT equations. Our obtained results remain

qualitatively similar for any symmetric DOS representing a bipartite lattice. This is in particular true for the three-dimensional cubic lattice, which has only mild Van Hove singularities. For fermionic DMFT it has been established that the agreement between results on the Bethe lattice and the cubic lattice is not only qualitative, but also quantitative, with a typical accuracy of around ten percent. We find that the same is true for BDMFT, as we show below for the case of single component bosons, where we compare the BDMFT results with numerically exact quantum Monte Carlo results.

In deriving the effective impurity action, we first formally rescale all hopping parameters as $t_{\nu} = t_{\nu}^* / z$, such that $1/z$ appears as the small parameter in the theory. Based on the linked cluster theorem, the action of the impurity site up to subleading order in $1/z$ is then obtained in the standard way¹⁵ as

$$S_{\text{imp}} = \int_0^{\beta} d\tau d\tau' \sum_{\mu\nu} \begin{pmatrix} b_{0\mu}^*(\tau) \\ b_{0\mu}(\tau) \end{pmatrix}^T \begin{pmatrix} (\partial_{\tau'} - \mu_{\mu}) \delta_{\mu\nu} + t_{\mu} t_{\nu} \sum_{\langle 0i \rangle, \langle 0j \rangle} G_{\mu\nu,ij}^1(\tau, \tau') & t_{\mu} t_{\nu} \sum_{\langle 0i \rangle, \langle 0j \rangle} G_{\mu\nu,ij}^2(\tau, \tau') \\ t_{\mu} t_{\nu} \sum_{\langle 0i \rangle, \langle 0j \rangle} G_{\mu\nu,ij}^{2*}(\tau', \tau) & (-\partial_{\tau'} - \mu_{\mu}) \delta_{\mu\nu} + t_{\mu} t_{\nu} \sum_{\langle 0i \rangle, \langle 0j \rangle} G_{\mu\nu,ij}^1(\tau', \tau) \end{pmatrix} \begin{pmatrix} b_{0\nu}(\tau') \\ b_{0\nu}^*(\tau') \end{pmatrix} \\ + \int_0^{\beta} d\tau \left\{ \frac{1}{2} \sum_{\nu\mu} U_{\nu\mu} n_{0\nu}(\tau) [n_{0\mu}(\tau) - \delta_{\nu\mu}] - \sum_{\langle 0i \rangle, \nu} t_{\nu} [b_{0\nu}^*(\tau) \phi_{i,\nu}(\tau) + b_{0\nu}(\tau) \phi_{i,\nu}^*(\tau)] \right\}. \quad (3)$$

Here we have defined

$$\phi_{i,\nu}(\tau) = \langle b_{i,\nu}(\tau) \rangle_0, \quad (4)$$

as the superfluid order parameters, and

$$G_{\mu\nu,ij}^1(\tau, \tau') = -\langle b_{i,\mu}(\tau) b_{j,\nu}^*(\tau') \rangle_0 + \phi_{i,\nu}(\tau) \phi_{j,\mu}^*(\tau'), \quad (5)$$

$$G_{\mu\nu,ij}^2(\tau, \tau') = -\langle b_{i,\mu}(\tau) b_{j,\nu}(\tau') \rangle_0 + \phi_{i,\nu}(\tau) \phi_{j,\mu}(\tau'), \quad (6)$$

as the diagonal and off-diagonal parts of the connected Green’s functions, respectively. The notation $\langle \dots \rangle_0$ means that the expectation value is taken in the cavity system excluding the impurity site. For finite z the action (3) coincides with the one previously derived in Ref. 16. Note however, that our derivation is different. In the original proposal,¹⁶ BDMFT is constructed as a well-defined theory in strictly infinite dimensions, which requires different scaling of superfluid and normal parts of the action. In contrast, our derivation is based on a uniform scaling $\sim 1/z$ of the bosonic hopping amplitude, since we focus on finite dimensions and our goal is to make direct contact with the three-dimensional experimental situation. The terms involving Green’s functions in the action (3) are of order $O(1/z)$, since they come with two factors of $t_{\nu} \sim 1/z$ and one summation over neighboring sites, which gives a factor z . All the other terms are of order $O(1)$; for the last term in the action this follows from the fact that it involves one factor of $t_{\nu} \sim 1/z$ which cancels against the factor z arising from the summation over neigh-

boring sites. Therefore to leading order the action (3) yields Gutzwiller mean-field theory,⁶ while by including the subleading terms of order $O(1/z)$ we obtain the BDMFT equations. Hence we regard BDMFT as an expansion in $1/z$ around Gutzwiller; this is in our opinion the most natural viewpoint.

To proceed, expectation values in the cavity system need to be identified with those on the impurity site, in order to obtain a closed self-consistency loop. Since sites at the edge of the cavity have one neighbor less compared to the impurity site (see Fig. 1), simply identifying the expectation values yields an error of order $1/z$. For the Green’s functions this poses no problem, because they already appear at subleading order in the action, but it yields a relevant correction to the superfluid order parameter and turns out to be essential

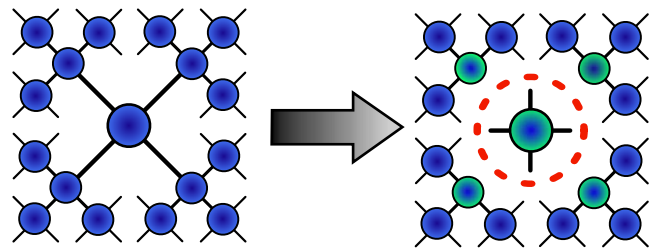


FIG. 1. (Color online) Illustration of the cavity method. Sites which are connected to the impurity (colored greenish) have one neighbor less once the impurity is removed.

for quantitatively accurate predictions of the phase diagram. Details regarding the implementation will be given below.

We now turn to the solution of the effective action. This we do in the spirit of the exact diagonalization (ED) solution of fermionic DMFT.¹⁵ We represent the effective action (3) by an Anderson impurity Hamiltonian \hat{H}_A :

$$\begin{aligned} \hat{H}_A = & - \sum_{\nu} z t_{\nu} (\phi_{\nu}^* \hat{b}_{\nu} + \text{h.c.}) + \frac{1}{2} \sum_{\nu\mu} U_{\nu\mu} \hat{n}_{\nu} (\hat{n}_{\mu} - \delta_{\nu\mu}) - \sum_{\nu} \mu_{\nu} \hat{n}_{\nu} \\ & + \sum_l \epsilon_l \hat{a}_l^{\dagger} \hat{a}_l + \sum_{l,\nu} (V_{\nu,l} \hat{a}_l^{\dagger} \hat{b}_{\nu} + W_{\nu,l} \hat{a}_l \hat{b}_{\nu} + \text{H.c.}). \end{aligned} \quad (7)$$

The chemical potential and interaction term are directly inherited from the Hubbard Hamiltonian. The Gutzwiller term represents the bath of condensed bosons with superfluid order parameters ϕ_{ν} for every component. The bath of normal bosons is modeled by a finite number of orbitals with creation operators \hat{a}_l^{\dagger} and energies ϵ_l . These orbitals are coupled to the impurity via normal-hopping amplitudes $V_{\nu,l}$ and anomalous-hopping amplitudes $W_{\nu,l}$. The anomalous hopping terms are needed to generate the off-diagonal elements of the hybridization function. We define the following hybridization functions:

$$\Delta_{\nu\mu}^1(i\omega_n) \equiv - \sum_l \frac{V_{\nu,l} V_{\mu,l}}{\epsilon_l - i\omega_n} + \frac{W_{\nu,l} W_{\mu,l}}{\epsilon_l + i\omega_n}, \quad (8)$$

$$\Delta_{\nu\mu}^2(i\omega_n) \equiv - \sum_l \frac{V_{\nu,l} W_{\mu,l}}{\epsilon_l - i\omega_n} + \frac{V_{\nu,l} W_{\mu,l}}{\epsilon_l + i\omega_n}. \quad (9)$$

Integrating out the orbitals leads to the same effective action (3), if the following identification is made:

$$z t_{\nu} t_{\mu} G_{\nu\mu}^{1,2}(i\omega_n) \hat{=} \Delta_{\nu\mu}^{1,2}(i\omega_n). \quad (10)$$

These self-consistency conditions are completed by the condition for the superfluid order parameter

$$\phi_{\nu} = \langle \hat{b}_{\nu} \rangle_0^{z-1}. \quad (11)$$

The notation $\langle \dots \rangle_0^{z-1}$ means that the expectation value is corrected for the missing neighbor on the sites adjacent to the impurity. Since this is a correction of order $O(1/z)$ and $1/z$ is small, this correction is implemented by means of perturbation theory in $1/z$. Equations (10) and (11) thus constitute the set of BDMFT self-consistency conditions.

The self-consistency loop is solved as follows: starting from an initial choice for the superfluid order parameter and the Anderson parameters, the Anderson Hamiltonian is constructed in the Fock basis and diagonalized to obtain the eigenstates and eigenenergies. New superfluid order parameters are then obtained from $\phi_{\nu} = \langle \hat{b}_{\nu} \rangle_0^{z-1}$. The eigenstates and energies also allow us to calculate the Green's functions. Subsequently, new Anderson parameters are obtained by fitting the hybridization functions to their corresponding Green's functions according to Eq. (10), which is done by a conjugate gradient method. With this new Anderson Hamiltonian the procedure is iterated until convergence is reached.

We note here that this derivation is independent of temperature. This implies that we cannot only determine ground

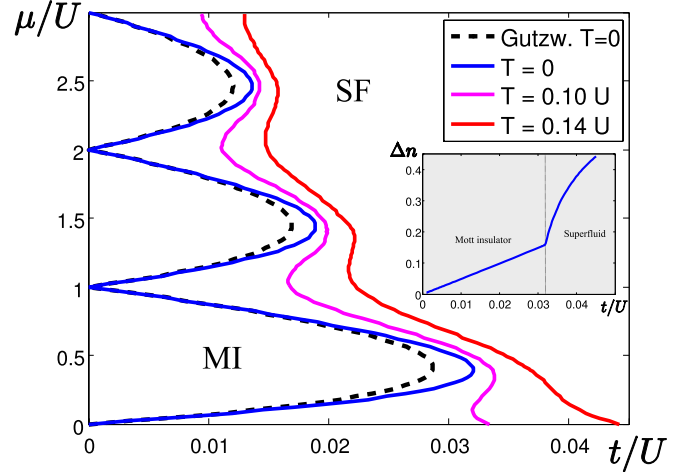


FIG. 2. (Color online) Single component phase diagram for various temperatures as obtained by BDMFT. In the inset: number fluctuations for density $n=1$ and $T=0$. The lattice coordination number is chosen as $z=6$.

state properties, but also obtain information about the thermodynamics of lattice bosons, as we will show in the following results. Similar to fermionic DMFT this raises the question how BDMFT deals with situations with broken symmetries, in which case Goldstone modes are present in the spectrum. Indeed, the gapless long wavelength excitations are absent from the DMFT spectrum.¹⁵ However, since in three dimensions the spectral weight of the Goldstone mode is finite and generally small, this approximation can be justified and does not prohibit qualitative agreement between (B)DMFT results and more exact methods (if available), even in symmetry-broken states.

III. RESULTS

A. Single component bosons

We now first apply BDMFT for the case of single component bosons, in which case we can compare the results with numerically exact quantum Monte Carlo data¹⁷ and strong coupling expansions^{18,19} on the cubic lattice, and with the exact solution on the Bethe lattice.²⁰ Solving the BDMFT equations for the single-component Bose-Hubbard model leads to an extension of the Mott-insulating lobes compared to the mean-field results (see Fig. 2). The agreement with the exact results on the Bethe lattice²⁰ is very good: for the lowest Mott lobe the phase boundaries agree within a few percent, whereas for the higher Mott lobes the agreement is even better. The predicted shift on the cubic lattice is slightly larger,¹⁷⁻¹⁹ which is due to the different lattice structure. This quantitative agreement with the exact solution clearly shows that the applied $1/z$ expansion is a very good approximation for a three-dimensional system with $z=6$. It is important to note that to obtain this result the $1/z$ correction of the superfluid order parameter discussed in the previous section is crucial.

Besides this quantitative agreement regarding the boundary of the Mott insulating lobes, it is also important to note

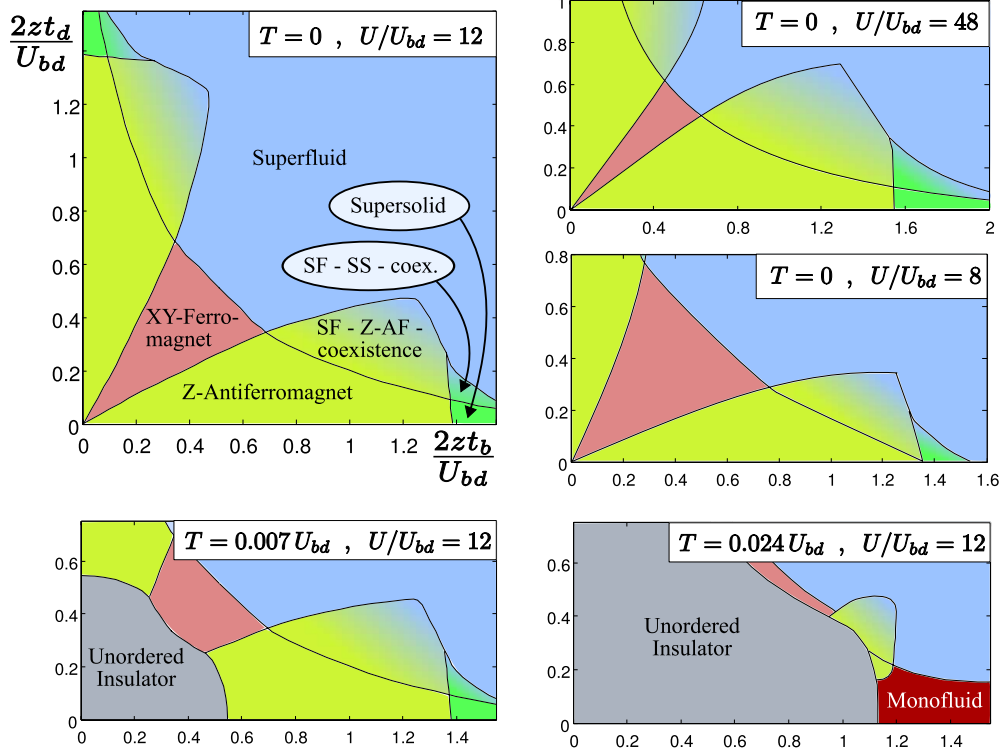


FIG. 3. (Color online) Phase diagram of a two-component bosonic mixture (in an optical lattice with $z=4$) at total density $n_1+n_2=1$ for different temperatures and ratios of the interspecies to the intraspecies interaction.

that BDMFT predicts nonzero number fluctuations in the Mott insulator, as shown in the inset of Fig. 2. The number fluctuations are clearly finite in the Mott state and decay as $1/U$ for large U . This is in contrast to the Gutzwiller mean-field result, where number fluctuations strictly vanish within the Mott state. Since these finite fluctuations in the Mott state are essential for resolving spin order in the case of multicomponent mixtures, spin order cannot be resolved within Gutzwiller. In contrast, the BDMFT contains number fluctuations in the Mott insulating state and is able to describe spin order as we describe in the following subsection.

B. Two-component bosons

The two-component Bose-Hubbard model has a very rich phase diagram, because additional spin order exists in the Mott phase. Here we focus on the situation that the total particle density is fixed at one boson per site. In the strong coupling limit, i.e., for $t_v \ll U_{\mu\nu}$, the system can be mapped to a spin model, which predicts the existence of a Z-antiferromagnet and a XY-ferromagnetic phase.^{7,8} In terms of the particle creation/annihilation operators \hat{b}_1, \hat{b}_2 , all the insulating phases have the property that $\langle \hat{b}_1 \rangle = \langle \hat{b}_2 \rangle = 0$. The Z-antiferromagnetic phase breaks the translational symmetry and is defined by the antiferromagnetic order parameter $\Delta_{\text{af}}^\mu = |n_{\alpha,\mu} - n_{\bar{\alpha},\mu}|$ being nonzero, where μ denotes the component and α ($\bar{\alpha} = -\alpha$) the sublattice. The correlator $\langle \hat{b}_1^\dagger \hat{b}_2 \rangle$ vanishes in the Z-antiferromagnetic phase. The XY-ferromagnet is defined by the local correlator $\langle \hat{b}_1^\dagger \hat{b}_2 \rangle$ being nonzero, and is also

termed a counterflow superfluid. This state does not break the translational symmetry and hence $\Delta_{\text{af}}^\mu = 0$.

At weaker coupling the spin model breaks down, because quantum fluctuations become important. A fluctuation calculation⁹ and strong coupling expansion¹⁰ have extended the spin model results to weaker coupling, where a transition to a superfluid phase $\langle \hat{b}_1 \rangle, \langle \hat{b}_2 \rangle \neq 0$ takes place. The superfluid does not break the translational symmetry ($\Delta_{\text{af}}^\mu = 0$) but shows XY ordering: $|\langle \hat{b}_1^\dagger \hat{b}_2 \rangle| > |\langle \hat{b}_1 \rangle \langle \hat{b}_2 \rangle|$.

We now investigate this system by means of BDMFT which allows us to study the full range from weak to strong coupling and effects of finite temperature. We first study the case that the intraspecies interactions $U=U_1=U_2$ are equal and much larger than the interspecies interaction $U_{12} \ll U$. We moreover vary the hopping amplitudes t_1 and t_2 . The condition $n_b+n_d=1$ is enforced by the choice of the chemical potential $\mu_1=\mu_2=U_{12}/2$. This has the consequence that the relative density of the two components is changing throughout the phase diagram: the species with a higher hopping constant (the light species) has a slightly higher density in the superfluid phases of the phase diagram. In the insulating phases, on the other hand, the Mott gap protects the particle number and the relative densities are to a good approximation equal. Results are presented in Fig. 3 for various ratios U/U_{12} . For easy comparison with Ref. 14 here $z=4$ is chosen. In agreement with the fluctuation calculation⁹ we obtain a XY-ferromagnetic state when the hopping amplitudes are comparable. This XY-ferromagnetic domain shrinks if U/U_{12} becomes larger. For a larger difference between the hopping amplitudes there is a first order phase transition toward a Z-antiferromagnetic state. The XY-ferromagnetic to super-

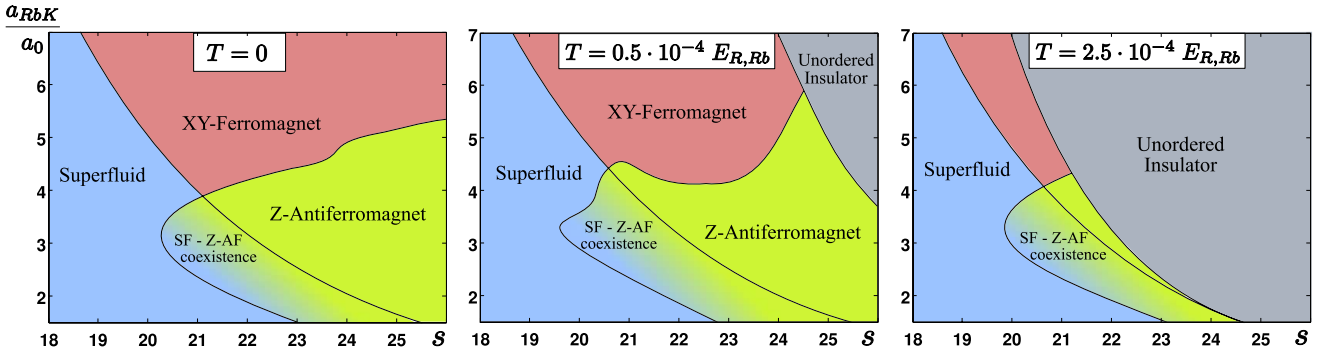


FIG. 4. (Color online) Phase diagram of a ^{87}Rb - ^{41}K mixture (for $z=6$) at fixed total density $n_{\text{Rb}}+n_{\text{K}}=1$ as a function of lattice depth s and Rb-K scattering length in units of the Bohr radius.

fluid transition is of second order, while on the other hand the Z-antiferromagnet to superfluid transition is first order, which is the reason for the large coexistence regions where both Z-antiferromagnetic order and superfluidity are stable/metastable, depending on the initial conditions. Within these metastable regions, patches with ground state spin order will nucleate into the metastable background. Therefore this phase will be susceptible to the appearance of quantum emulsions, as predicted for a one-dimensional Bose-Bose mixture.²¹ However, this phenomenon is expected to be much more prominent in one dimension than in the three-dimensional situation we consider.

For very anisotropic hopping amplitudes, we predict the appearance of a supersolid phase. In this supersolid the species with the smaller hopping amplitude (for convenience we take this as species 2, i.e., $t_1 \gg t_2$) is insulating: $\langle \hat{b}_2 \rangle = 0$, whereas the other component (i.e., species 1) is superfluid: $\langle \hat{b}_1 \rangle \neq 0$. Moreover the complete system breaks translational symmetry by developing a spin density wave, in which both components have alternating high and low on-site densities: $\Delta_{\text{af}}^\mu > 0$, for $\mu=1, 2$.

Since the light species breaks the U(1) and translational symmetries simultaneously, this phase is a true supersolid. The breaking of the translation symmetry is mediated by the presence of the heavy species, akin to the situation in a Bose-Fermi mixture, where supersolid order has been predicted as well.^{22,23} The supersolid has a first-order transition to the superfluid and a second-order phase transition to the Z antiferromagnet. The latter one can be understood as the localization transition of the light component. The supersolid phase has not been predicted in earlier studies on Bose-Bose mixtures.^{9,10} Only very recently it was observed in a quantum Monte Carlo (QMC)-analysis for the two-dimensional case.¹⁴

For nonzero temperatures additional quantum phases appear (see Fig. 3). At low temperatures the XY ferromagnet and Z antiferromagnet in low-hopping regions develop into an unordered Mott-state with $\langle \hat{b}_\mu \rangle = \langle \hat{b}_1^\dagger \hat{b}_2 \rangle = \Delta_{\text{af}}^\mu = 0$. The coexistence regions and insulator-to-superfluid transitions remain unaffected. For higher temperatures the XY-insulating phase is reduced to a small strip between the growing unordered phase and the receding superfluid. The Z-antiferromagnetic and the AF-SF-coexistence region diminish considerably. For certain parameters the counterintui-

tive phenomenon of reentrant superfluidity takes place: the low-temperature antiferromagnetic phases become superfluid when the temperature is increased. This is the case because the superfluid is more stable against temperature fluctuations than the insulating Z antiferromagnet. If the temperature is increased in the region of stability of the supersolid, first the translational symmetry is restored: we obtain a phase in which only the light component is superfluid ($\langle \hat{b}_1 \rangle \neq 0$, $\langle \hat{b}_2 \rangle = 0$), but which has no broken translational symmetry ($\Delta_{\text{af}}^\mu = 0$) in contrast to the supersolid. We call this phase *monofluid*. Upon further increasing the temperature, also the remaining superfluid order is lost.

C. Rubidium-potassium mixture

Up to now, theoretical calculations were mainly performed for the symmetric parameter choice $U_b = U_d$. However, the experimentally at present most relevant Bose-Bose mixture consisting of ^{87}Rb and ^{41}K generally does not have this property.^{3,4} Here we choose the wavelength of the optical lattice equal to $\lambda = 757$ nm, which yields equal dimensionless lattice depths $s = V_0/E_R$ for the two species. E_R is the recoil energy and V_0 is the strength of the optical potential, which is proportional to the product of laser intensity and atomic polarizability. The ratio of the intraspecies interaction parameters is then fixed according to $U_{\text{Rb}}/U_{\text{K}} = m_{\text{K}}a_{\text{Rb}}/m_{\text{Rb}}a_{\text{K}} \approx 0.72$. The ratio of the hopping coefficients is also fixed: $t_{\text{Rb}}/t_{\text{K}} = m_{\text{K}}/m_{\text{Rb}} \approx 0.47$. This choice of the wavelength turns out to be sufficiently anisotropic to show both XY order and antiferromagnetic order, which is not possible for mixtures of different hyperfine states of the same atom. Choosing the wavelength far red detuned like in Ref. 3 on the other hand, excludes the XY phase from the phase diagram, but makes it possible to study the antiferromagnet and supersolid.

Experimentally, the ratio of intraspecies interaction to interspecies interaction can be tuned via Feshbach-resonances.⁴ Furthermore the optical lattice depth s can be changed to tune the ratio $U_{\text{Rb}}/t_{\text{Rb}}$. We investigate the resulting s - a_{RbK} phase diagram at fixed total density $n_{\text{Rb}}+n_{\text{K}}=1$ by means of BDMFT, still using the semicircular DOS, but taking now lattice coordination number $z=6$ as corresponding to the three-dimensional situation. Results are shown in Fig. 4. This mixture displays superfluid, XY-ferromagnetic and

Z-antiferromagnetic phases and we also observe the hysteresis (metastable) region between superfluid and antiferromagnet. For nonzero temperatures and high lattice depths the unordered Mott-state appears. At the temperature $T=2.5 \times 10^{-4} E_{R,Rb}$, ($E_{R,Rb}$ being the recoil energy of rubidium), the ordered insulating states are reduced to a small part of parameter space, which is diminished even further for higher temperatures. In order to compare this temperature to the temperatures reached in recent experiments, we consider a simple model of free bosons that undergo adiabatic time evolution while the optical lattice is ramped up. We obtain an estimate for the temperature at the relevant lattice depth in the Florence group that is one order of magnitude larger than the highest temperature investigated here.³ Recent direct measurements of the temperature of a spinful bosonic mixture in an optical lattice at MIT have yielded temperatures which correspond to only twice the highest temperature we consider.²⁴

The phase diagrams in Fig. 4 are valid for the case of a shallow harmonic trap, where in the trap center the potential is very flat. Moreover, the two species need to be equally distributed in the trap center, which means that the gravitational sag has to be compensated.

IV. CONCLUSIONS

We have derived bosonic DMFT within a $1/z$ expansion and extended the formalism to the full multicomponent

Bose-Hubbard model in finite dimensions. We first validated the method by applying it to spinless bosons. Qualitative and quantitative agreement with other methods was established. Subsequently we investigated a two-component mixture. We applied the method to a two-component mixture. A rich phase diagram including spin-ordered and supersolid phases was found. We furthermore calculated the experimentally relevant phase diagrams for a ^{87}Rb - ^{41}K in an optical lattice at zero and finite temperature.

Note added. Recently, the BDMFT equations were also solved for the single-component Bose-Hubbard model in infinite dimensions, using a similar Anderson Hamiltonian and the same Exact Diagonalization approach as originally proposed by us.²⁵

ACKNOWLEDGMENTS

We thank K. Byczuk, D. Vollhardt, and F. Minardi for useful discussions. This work was supported by the German Science Foundation DFG via Forschergruppe FOR 801 and Sonderforschungsbereich SFB/TRR 49 and by the Nederlandse Organisatie voor Wetenschappelijk Onderzoek (NWO).

-
- ¹M. P. A. Fisher, P. B. Weichman, G. Grinstein, and D. S. Fisher, Phys. Rev. B **40**, 546 (1989).
²D. Jaksch, C. Bruder, J. I. Cirac, C. W. Gardiner, and P. Zoller, Phys. Rev. Lett. **81**, 3108 (1998).
³J. Catani *et al.*, Phys. Rev. A **77**, 011603(R) (2008).
⁴G. Thalhammer, G. Barontini, L. De Sarlo, J. Catani, F. Minardi, and M. Inguscio, Phys. Rev. Lett. **100**, 210402 (2008).
⁵S. Trotzky *et al.*, Science **319**, 295 (2008).
⁶D. S. Rokhsar and B. G. Kotliar, Phys. Rev. B **44**, 10328 (1991); K. Sheshadri, H. R. Krishnamurthy, R. Pandit, and T. V. Ramakrishnan, Europhys. Lett. **22**, 257 (1993).
⁷A. B. Kuklov and B. V. Svistunov, Phys. Rev. Lett. **90**, 100401 (2003).
⁸L.-M. Duan, E. Demler, and M. D. Lukin, Phys. Rev. Lett. **91**, 090402 (2003).
⁹E. Altman, G. Meyer, S. M. Stojkovic, A. Gourdon, and C. Joachim, New J. Phys. **5**, 113 (2003).
¹⁰A. Isacsson, Min-Chul Cha, K. Sengupta, and S. M. Girvin, Phys. Rev. B **72**, 184507 (2005).
¹¹S. Powell, Phys. Rev. A **79**, 053614 (2009).
¹²O. E. Alon, A. I. Streltsov, and L. S. Cederbaum, Phys. Rev. Lett. **97**, 230403 (2006).
¹³A. Kleine, C. Kollath, I. McCulloch, T. Giamarchi, and U. Schollwoeck, Phys. Rev. A **77**, 013607 (2008).
¹⁴S. G. Söyler, B. Capogrosso-Sansone, N. V. Prokof'ev, and B. V. Svistunov, New J. Phys. **11**, 073036 (2009).
¹⁵W. Metzner and D. Vollhardt, Phys. Rev. Lett. **62**, 324 (1989); A. Georges, Gabriel Kotliar, Werner Krauth, and Marcelo J. Rozenberg, Rev. Mod. Phys. **68**, 13 (1996).
¹⁶K. Byczuk and D. Vollhardt, Phys. Rev. B **77**, 235106 (2008).
¹⁷B. Capogrosso-Sansone, N. V. Prokof'ev, and B. V. Svistunov, Phys. Rev. B **75**, 134302 (2007).
¹⁸F. E. A. dos Santos and A. Pelster, Phys. Rev. A **79**, 013614 (2009).
¹⁹M. Ohliger and A. Pelster, arXiv:0810.4399 (unpublished).
²⁰G. Semerjian, M. Tarzia, and F. Zamponi, Phys. Rev. B **80**, 014524 (2009).
²¹T. Roscilde and J. I. Cirac, Phys. Rev. Lett. **98**, 190402 (2007); P. Buonsante, S. M. Giampaolo, F. Illuminati, V. Penna, and A. Vezzani, *ibid.* **100**, 240402 (2008).
²²H. P. Büchler and G. Blatter, Phys. Rev. Lett. **91**, 130404 (2003).
²³I. Titvinidze, M. Snoek, and W. Hofstetter, Phys. Rev. Lett. **100**, 100401 (2008).
²⁴D. M. Weld, P. Medley, H. Miyake, D. Hucul, D. E. Pritchard, and W. Ketterle, Phys. Rev. Lett. **103**, 245301 (2009).
²⁵W.-J. Hu and N.-H. Tong, Phys. Rev. B **80**, 245110 (2009).